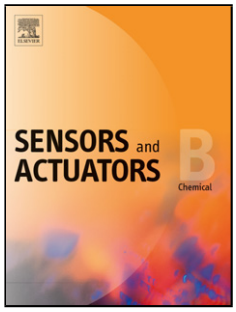

Title: Ultrasensitive Dynamic Light Scattering based Nanobiosensor for Rapid Anticancer Drug Screening

Authors: Xin Ting Zheng, Walter L. Goh, Peter Yeow, David P. Lane, Farid J. Ghadessy, Yen Nee Tan

PII: S0925-4005(18)31723-4
DOI: https://doi.org/10.1016/j.snb.2018.09.088
Reference: SNB 25394

To appear in: *Sensors and Actuators B*

Received date: 22-5-2018
Revised date: 20-9-2018
Accepted date: 22-9-2018

Please cite this article as: Ting Zheng X, Goh WL, Yeow P, Lane DP, Ghadessy FJ, Nee Tan Y, Ultrasensitive Dynamic Light Scattering based Nanobiosensor for Rapid Anticancer Drug Screening, *Sensors and amp; Actuators: B. Chemical* (2018), https://doi.org/10.1016/j.snb.2018.09.088

Ultrasensitive Dynamic Light Scattering based Nanobiosensor for Rapid Anticancer Drug Screening

Xin Ting Zheng [a,‡], Walter L. Goh [b,‡], Peter Yeow [b], David P. Lane [b], Farid J. Ghadessy [b] and Yen Nee Tan [a,c*]

[a] Institute of Materials Research and Engineering (IMRE) , Agency for Science, Technology and Research (A*STAR), 2 Fusionopolis Way, 138634, Singapore
[b] p53 Laboratory, 8A Biomedical Grove, #06-04/05 Neuros/Immunos, 138648, Singapore
[c] Chemical Engineering, Newcastle University, 537 Clementi Road #06-01, 599493 Singapore

*Corresponding author. T el: +65 64168969
E-mail: tanyn@imre.a-star.edu.sg ; yennee.tan@ncl.ac.uk (Y.N. Tan)

Graphical Abstract

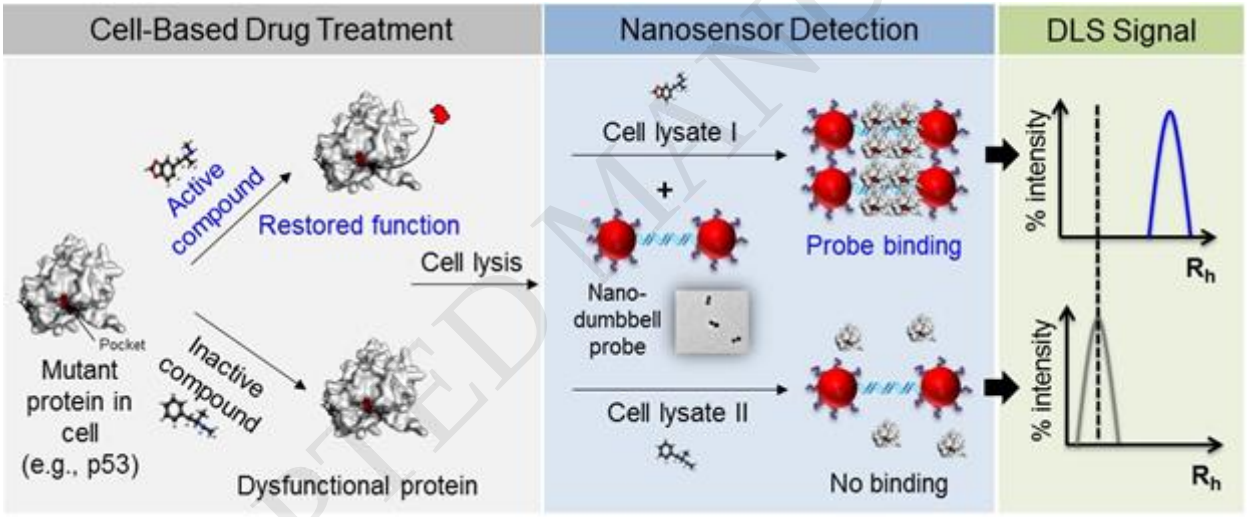

Highlights

- Ultrasensitive DLS-based nanobiosensor for drugs screening in cellular context
- Detection based on hydrodynamic size changes of gold-nanodumbell probes upon drug-protein-DNA binding interactions
- Nanoplasmonic biosensing probes enabled high specificity and low background noise
- Rapid competition assay for determining relative binding affinities and drug activation pathways
- Broadly applicable nanobiosensor concept for DNA-binding molecules and drug study

ABSTRACT

Improved chemical library screens for drug modulators of a target protein are vital to advance precision medicine. Here, we describe an ultrasensitive dynamic light scattering (DLS) based biosensor using gold nanoparticles as plasmon-enhanced sensing probes to rapidly screen anticancer compounds. The nanobiosensor which consists of DNA-conjugated dumbbell-shaped gold nanoprobes can detect protein activities in drug-treated cells. We have validated the utility of our nanosensor to screen for compounds known to reactivate mutated tumor suppressor protein p53 for DNA binding in complex cellular context, which leads to significant increases in the hydrodynamic size of the nanoprobes through DLS measurement. This unique nanoplasmonic biosensor not only significantly enhances the DLS signal for specific biomolecular binding, but also effectively suppresses the background noise from irrelevant entities, which greatly improves sensitivity and reduces consumption of both sample and probe. In addition, a competition assay designed to evaluate the relative DNA binding affinities of p53 using the same sensing probes allows a concomitant assessment of responsive p53 pathways downstream or cell fate. Most critically, this nanosensor enables direct interrogation of endogenous protein activities following drug treatment in live cells, allowing simultaneous on-target validation during phenotypic screens. This DLS-based nanobiosensor is broadly applicable to other DNA binding molecules and/or proteins, and holds great potential for high-throughput screening campaigns utilizing both conventional and fragment-based compound libraries in drug discovery.

Keywords: nanobiosensor; dynamic light scattering; drug screening; gold nanoparticles; anticancer drug; cell lysate

1. Introduction

The therapeutic effect of most clinical drugs is achieved through target binding with subsequent modulation of protein activity in a cellular context which leads to the desired therapeutic responses [1]. The two main approaches for drug discovery include target-based biochemical screening and phenotypic cell-based screening [2]. Target-based assays typically measure drug-target engagement using purified proteins but may not be relevant to the disease pathogenesis in cellular contexts. On the other hand, cell-based assays usually detect observable changes in cell physiology without target validation or identification of molecular mechanisms of action. This leads to significant challenges to optimization of the molecular properties of candidate drugs. These problems have led to the failure of many drugs in advanced clinical trials as the drug candidates did not act on intended intracellular targets [3, 4]. Thus, it is critical to develop a sensing platform that evaluates drug-modulated target protein activity in a cellular environment for early validation of drug candidates before significant investments in clinical trials.

Cancer is the leading cause of death despite decades of intensive research on anticancer therapeutics development. Among the various cancer related drug targets, the p53 tumor suppressor protein [5] is a prime target for cancer therapy development [6, 7] and was chosen as a model protein target for nanosensor development in this study. As a master transcription factor, p53 binds to specific DNA response elements (REs) that regulate target genes involved in cellular processes such as DNA repair, cell cycle arrest or apoptosis [8]. Mutations in the *TP53* gene occur in over 50% of all human cancers and the majority of cancer-associated p53 mutations occur within the DNA-binding core domain, resulting in mutant proteins with structural defects and DNA-binding impairments [9]. Targeted hyper-degradation of p53 is also associated with malignancy [5].

Thus far, a variety of techniques including electrophoretic mobility shift assay (EMSA) [10], fluorescence anisotropy [11, 12], Surface Plasmon Resonance (SPR) [13, 14], and enzyme-linked immunosorbent assay (ELISA) [15] have been developed for p53 detection.

These methods face many drawbacks of being heterogeneous-phase assays that require multiple technically challenging surface treatments, expensive reagents/instrumentation, and thus cannot readily be used for drug screening. Furthermore, signal-to-noise constraints preclude the use of complex cellular lysates, a requirement crucial for the activity of prodrugs or compounds that require an intact intracellular environment to function. Other techniques like the qPCR-based p53-DNA binding assay [16], microsphere assay for protein-DNA binding (MAPD) [17], electrochemical sensor [18-21] or chemiluminescence detection [22, 23] afford increased sensitivity and compatibility with complex solutions, but still face caveats in assay complexity, high reagent costs and limited throughput. The lack of appropriate p53-interrogative platforms in drug screening campaigns has also led to early termination of clinical drug candidates due to associated off-target toxicities. Therefore, development of a sensitive nanosensor for rapid screening of p53 modulators is of high clinical value and will be vital to advancing precision medicine.

Dynamic light scattering (DLS) is a well-known analytical technique for particle size analysis, and is routinely used in laboratories to determine the sizes of biomolecules and also in the pharmaceutical industry to study drug formulation. Most biomolecules scatter light very weakly, so usually highly purified proteins at micromolar concentrations are required to characterize their hydrodynamic sizes [24]. Furthermore, since proteins and nucleic acids all scatter light to similar extents, it is almost impossible to distinguish between different biomolecules and examine their interactions using conventional DLS. Gold nanoparticles (AuNPs), on the other hand, exhibit large light scattering cross-section (200-300 times stronger than that of polystyrene beads and 10^6-fold stronger than that of a fluorescent dye) due to the localized Surface Plasmon Resonance (LSPR) effect that can enhance DLS signal and suppresses background noise [19]. Recently, biofunctionalised AuNPs have emerged as signal amplification probes for DLS-based sensitive detection of DNA [25], proteins [26-29], bacteria

[30] and small molecules [31, 32]. However, to the best of our knowledge, a DLS based nanosensor for rapid drug screening has not been reported.

In this study, we report a facile, robust, and effective approach for anticancer drug screening based on a nanoplasmonic sensor by DLS signal measurements. This nanosensor is capable of detecting sequence-specific p53-DNA binding in real-time, quantifying functional p53 in cell lysates, and directly interrogating p53 activation or reactivation following drug treatment in live cells. This nanosensor marries the benefits of both target-based and cell-based drug screening approaches, allowing the validation of target protein function and therapeutic cellular response within the same sample. Furthermore, the nanosensor can be applied in a competition assay to evaluate relative DNA binding affinities for downstream pathway and cellular response determinations using a single set of probes. We successfully demonstrate the detection of canonical DNA binding using endogenous p53 proteins expressed in cells treated with conventional cancer drugs or experimental compounds targeting mutant or wildtype p53, providing the basis for applications in drug design and chemical library screens. The nanosensor enables fast (< 5 min) and "mix-and-measure" screening of anticancer compounds in multi-well plates, and will be of great use in high-throughput drug screening campaigns.

2. Materials and methods

2.1. Reagents and buffers

Hydrogen tetrachloroaurate (III) trihydrate ($HAuCl_4$), trisodium citrate dihydrate, tannic acid, *4,4'* (Phenylphosphinidene)bis (benzenesulfonic acid) dipotassium salt hydrate 97% (PPBS), NaCl, $MgCl_2$, and Tris-Borate-EDTA (TBE) buffer were purchased from Sigma-Aldrich. Tris buffer (pH 8), agarose powder, and synthetic DNA sequences with or without thiol modifications (Supporting information, **Table S1 & S2**) were ordered from Integrated DNA Technologies Pte Ltd. The recombinant p53 proteins were expressed and purified as described in supporting information. The ultrapure water was obtained from a Millipore Milli-Q water purification system and used throughout the experiments.

2.2. Fabrication of nanosensor

AuNPs were synthesized by the reduction of $HAuCl_4$ using trisodium citrate and tannic acid as described by Handley *et al*. [33]. The as-synthesized AuNPs were first passivated with 80 mM PPBS for at least 4 h to gain necessary stability in a mild salt concentration. The PPBS-passivated AuNPs were washed with 1 M Tris buffer and then centrifuged to remove excess PPBS. The PPBS-passivated AuNPs were incubated with one of three single-stranded DNA (ssDNA) - Seq A, B or C (**Table S1**) for 3 h, followed by passivation with 5' thiolated 5-T ssDNA (5'-thiol-TTTTT) overnight. The NaCl concentration of the system was gradually raised from 200 mM to 600 mM by adding a 5 M NaCl stock solution three times in 9 h. The ssDNA-conjugated AuNPs were washed with 50 mM Tris and NaCl buffer, and subsequently separated on a 3% agarose gel (75V, 180 min) using 0.5x TBE as running buffer. Desired bands were extracted from the gel to recover conjugate monomers bearing a single ssDNA [34-36]. The concentrations of the conjugate monomers were estimated using UV-*vis* spectrophotometer. Two sets of conjugate monomers (1 pmol each) were mixed in an annealing buffer containing 50 mM Tris (pH 8.0), 100 mM NaCl and 2 mM $MgCl_2$ and then hybridized to their complementary targets (i.e. seq A and B to seq AB; seq A and C to seq AC) at 1:1 conjugate monomer to target ratio. The hybridization of target DNA was carried out by first heating the mixture to 95^{o}C for 5 min and then slowly cooling down to 25^{o}C at a rate of 0.5^{o}C/min. The samples were eventually separated in a 3% agarose gel at 75V for 45 min to visualize the formation of nanosensors, which were subsequently recovered through the excision and dialysis of the desired gel band.

This as-synthesized nanosensor, also known as nano-dumbbell probe ($Probe_{\_RE}$) consists of two spherical AuNPs, bridged by a rigid double-stranded (ds)DNA sequence comprising of a p53 RE and its successful formation was confirmed by DLS and TEM measurements (**Fig. S1**).

2.3. DLS measurements for p53-DNA binding and competition assay

Purified wildtype or mutant p53 proteins were first mixed thoroughly with nano-dumbbell probes (Probe_RE, 0.3 nM) in p53 binding buffer (25 mM sodium phosphate, 150 mM KCl, pH 7.2) by pipetting. After incubation for specific durations, the mixtures were then transferred to a 384-well microplate and measured using a DLS plate reader (DynaPro™ plate reader, Wyatt technology). Subsequently, 10 measurements (~5 s each) were performed for each sample well. All binding experiments were performed in triplicates.

For competition assay, p53 proteins were first exposed to an excess of free dsDNAs (1 μM) comprising different p53 RE sequences as listed in **Table S2** for 5 min before mixing with Probe_RE for DLS measurements.

2.4. Cell culture, drug treatment and cell lysate preparation

H1299 cells stably integrated with the Ecdysone-Inducible system (H1299EI) [37] were made to express either wildtype, or mutant p53 (R273H, R175H, G245S) [38] in response to ponasterone-A (ThermoFisher Scientific). H1299EI cells and HCT-116 cells (ATCC® CCL-247™) were cultured in a 5% CO_2 environment, respectively in either DMEM/high glucose or McCoy's 5A media (Hyclone™, GE healthcare) supplemented with 10% fetal calf serum (GE healthcare) and 1x penicillin-streptomycin solution (Sigma Aldrich).

Cells seeded overnight are drug exposed the following day for 24 hours before being trypsin harvested. Harvested cells are then pelleted (900 x g, 3 min), resuspended in 700 μL of p53 binding buffer (25 mM phosphate buffer, 150 mM KCl, 2 mM DTT, pH 7.2) containing Pierce™ Phosphatase Inhibitor Mini Tablets (ThermoFisher Scientific) and cOmplete™ Mini EDTA-free Protease Inhibitor Cocktail Tablets (Sigma Aldrich), and subsequently lysed using a Dounce homogenizer with 200 passes on ice.

2.5. *Screening of p53-activating or reactivating compounds in cell lysates*

Crude lysates were centrifuged (15000 x g, 4°C) and supernatants were collected and diluted as desired (typically ~ 20 times) with p53 binding buffer. DO-1 antibody, a well-established and robust antibody for detecting human p53 proteins in cells was used in the

Western Blots to evaluate the p53 expression in cell lysates. Total protein content for each sample was first determined (BCA protein Assay Kit, ThermoFisher Scientific) and sample volumes were normalized by their total protein levels prior to mixing with nanosensors. The drug-treated cell lysates were then incubated with Probe$_{RE}$ before transferring to the 384-multiwell plate for DLS measurements.

3. Results and discussion

3.1. Principle of dynamic light scattering based nanosensor for drug screening

Scheme 1 illustrates the underlying principle for DLS based screening of anticancer drugs in homogenous solution using a unique nanosensor, which adopts a "dumbbell" shape of two AuNPs linked by a double-stranded (ds)DNA. The nano-dumbbell probe (Probe$_{PUMA}$) contains the physiological PUMA-BS2 response element (RE) in the dsDNA sequence to capture the p53 protein with high binding affinity (K_D = 7.1±1.8 nM) [39]. In this work, cells expressing mutant p53 proteins were incubated with drug candidates to screen for active compounds that restore the protein's native functions in cells. The cells were drug treated for 24 h and then lysed to obtain cell lysates. When lysates treated with active compounds were mixed with the nano-dumbbell probe, the reactivated p53 in the lysate was able to bind the DNA component of the nano-dumbbell probe, causing the hydrodynamic size to increase, and result in a distinct DLS peak right-shift. In contrast, if the p53 protein remains dysfunctional, it is not able to bind to the probe thus leading to insignificant change in hydrodynamic size. The extent of right-shifting of the DLS peak is indicative of drug efficacy. In this nanosensor, the DNA design with p53 RE allows sequence-specific detection of p53-DNA binding, while the strong light scattering of AuNPs helps to enhance the DLS signal and effectively suppresses the background noise from unbound molecules. Furthermore, each AuNP surface is passivated with a dense layer of short polythymine (polyT) oligonucleotides to effectively prevent non-specific adsorption of irrelevant biomolecules for complex sample detection.

3.2. Functionality of nanosensor: specificity, sensitivity and real-time detection

To demonstrate functionality of the nanosensor, we first measured the binding of purified wildtype p53 (wtp53) protein to the Probe_PUMA which contains the recognition sequence for p53 binding. A pronounce shift in the probe's DLS signature (indicative of increasing size) was observed in the presence of increasing amounts of wtp53, which suggests sequence-specific p53-DNA binding. It is known that wtp53 typically binds its REs as a tetramer [39], thus this significant increase in hydrodynamic size of the wtp53-bound Probe_PUMA is probably due to the "stacking" effect as four p53 monomers bind across separate and multiple Probe_PUMA which subsequently induces crosslinking and aggregation of Probe_PUMA (as depicted in Scheme 1). This phenomenon has also been observed in other studies [40, 41]. The "stacking" effect is further supported by the TEM evidence whereby clusters of AuNPs are observed in the sample of the wtp53-bound Probe_PUMA, with negligible free probes in the background (**Fig. S2**). Therefore, the probe-only peak at 30-40 nm disappears upon addition of wtp53, and the binding of increasing concentration of wtp53 proteins to Probe_PUMA is shown as the right-shift of a single DLS peak. A linear calibration plot (**Fig. 1a**) shows that the average hydrodynamic size of wtp53 bound Probe_PUMA is proportional to wtp53 concentration, with a linear range between 0-12 pM and an ultra-low detection limit of 0.06 pM (S/N=3).

To confirm that changes in DLS signal only come from on-target protein-DNA binding, wtp53 was also mixed with either unprotected citrate-anion capped AuNPs and/or short polyT passivated AuNPs. Heavy aggregation of citrate-anion capped AuNPs in the presence of wtp53, due to the non-specific protein adsorption onto the exposed AuNP surfaces, was entirely prevented with the polyT-oligonucleotide passivation (**Fig. S3**). Furthermore, a DLS peak shift was observed only when wtp53 was in the presence of Probe_PUMA carrying the intact double-stranded (ds)PUMA RE, but not the single-stranded (ss)DNA-AuNP conjugates, further

alluding to sequence-specific DNA binding. Zeta potentials were also measured to further explore the interaction between the wtp53 proteins and Probe_$_{PUMA}$. Since the zeta potentials of Probe_$_{PUMA}$ (-17.8±0.5 mV) and wtp53 (-8.3±2.7 mV) in binding buffer are both negative, there is no significant change in the zeta potential of the wtp53 bound Probe_$_{PUMA}$ (-18.3±3.4 mV).

To further ascertain canonical DNA-binding activity, DLS signal in response to wtp53 were compared between Probe_$_{PUMA}$ and non-binding control Probe_$_{Scr}$ (i.e., scrDNA sequence that does not contain the p53 RE). Both probes exhibit similar size distribution (~30 nm) in the absence of wtp53 protein, but only Probe_$_{PUMA}$ experiences increases in hydrodynamic size to ~150 nm upon wtp53 addition. No significant binding was observed between wtp53 and RE-lacking control probe, Probe_$_{Scr}$ (**Fig. 1b**), demonstrating high DNA sequence specificity. Furthermore, Probe_$_{PUMA}$ did not elicit signals in the presence of a DNA-binding compromised p53 mutant (mutp53$_{R273H}$), or non-relevant proteins such as BSA and HSA (**Fig. 1c**). When BSA was added in large molar excess (6.7 x 10^5-fold over wtp53) to either the Probe_$_{PUMA}$ alone, or the wtp53-bound Probe_$_{PUMA}$, no discrepancies in their size distribution (**Fig. 1d**) was observed, further highlighting high probe specificity and selectivity with effective background suppression.

Additionally, we discovered that Probe_$_{PUMA}$ can be utilized to monitor the protein-DNA binding kinetics in real-time, which is another invaluable feature for studying biomolecular interactions and affinity mechanisms. Here, wtp53 proteins were mixed with Probe_$_{PUMA}$ and DLS signals were acquired over multiple time points. On-target DLS signal can be observed within one minute (**Fig. 1e**) and increases till saturation at ~15 minutes. Furthermore, DLS signal intensities remain unchanged after two hours in solution, corroborating the stability and assay robustness of the wtp53-bound Probe_$_{PUMA}$ (**Fig. 1f**).

3.3. Competition assay for determination of relative DNA binding affinities

p53 transactivates gene targets through recognizing and binding a variety of experimentally verified DNA response elements [42-44]. A competition assay was designed to quickly determine the p53 protein's binding affinities to a variety of dsDNA REs using the same Probe_$_{PUMA}$. In this competition assay, binding of p53 proteins to Probe_$_{PUMA}$ was measured in the presence of excess free competing double-stranded oligonucleotides with varying p53-binding affinities (~3300-fold molar excess over Probe_$_{PUMA}$) (**Fig. 2a**). p53 proteins with higher affinity towards the free competing sequences in solution bind preferably to these sequences resulting in no change in the size of Probe_$_{PUMA}$. On the other hand, when the p53 proteins have lower affinity towards the competing sequences, they bind to Probe_$_{PUMA}$ preferentially leading to the right-shift of characteristic DLS peak. In this way, we are able to rank the relative binding affinities of p53 protein towards different DNA sequences. Competing DNA oligonucleotides used in our study include the p53 consensus sequence (ConA), two physiological p53-REs involved separately in regulating pro-apoptotic BAX and DNA-repair factor GADD45, and a p53 non-binding control DNA (Scr) (**Table S2**).

As shown in **Fig. 2b**, mixing of wtp53 with excess non-binding free Scr sequences exhibited similar levels of DLS signal to when no DNA competitor was added. However, when wtp53 was exposed to the high affinity ConA response element (K_D = 0.5 nM), almost no change in light scattering compared to Probe_$_{PUMA}$ alone was observed because wtp53 was predominantly sequestered onto ConA. Furthermore, hydrodynamic size changes of Probe_$_{PUMA}$ in the presence of other competing REs, i.e., GADD45 (K_D = 7.7 nM) and Bax (K_D = 77 nM), correlated well with their reported dissociation constants [12]. Critically, when the conserved core CATG binding motif within each decameric half-site of consensus RE (ConA) was mutated to **A**AT**T** (ConAmut), p53-ConAmut binding was greatly reduced as exemplified by the increase in p53-Probe_$_{PUMA}$ binding in agreement with previous reports [42], further demonstrating the dynamic nature of the assay. This competition assay can be further applied to evaluate the relative DNA binding affinities of drug reactivated proteins, thus allowing the

prediction of the downstream pathways reactivated upon DNA binding and consequently the cell fate (cell cycle arrest, DNA repair, senescence or apoptosis).

3.4. Detection of protein oligomerization

Typically, wildtype p53 binds REs as a tetramer through the association of each monomeric subunit with a 5-bp quarter-site within the 20-bp RE [39]. Cells carrying both functional and mutant p53 alleles (germline heterozygous or somatic mutated) can experience an attenuated p53 response from compromised DNA-binding through the formation of mutant-wildtype hetero-tetramers or -dimers [45]. This dominant-negative effect of mutant p53 was recapitulated when wtp53 and mutp53$_{R273H}$ were mixed at varying proportions before exposure to Probe$_{_PUMA}$. A significant reduction in binding was observed at equimolar proportions (wtp53: mutp53$_{_R273H}$ = 1:1), with a complete ablation of DNA-binding when mutant proteins were present in two-fold excess (wtp53: mutp53$_{_R273H}$ = 1:2) (**Fig. 2c**). The presence of mutant protein in the sample disrupts the formation of wildtype homodimers which subsequently hinders the formation of a stable wildtype tetramer leading to signal suppression. However, in the absence of preincubation step to permit heterodimer formation, little effect on the overall binding was observed, even when mutant proteins were present at 10-fold molar excess (wtp53: mutp53$_{_R273H}$ = 1:10) (**Fig. 2d**). This result highlights the additional utility for studying protein biochemistry. Most importantly, this result shows that tetramerization of four wtp53 monomers is essential for wtp53-Probe$_{_PUMA}$ complex stabilization and subsequent stacking to give a significant DLS peak shift. From here, we deduce that two types of biomolecular interactions play critical roles in protein-probe interaction including both protein-protein interaction (i.e. tetramerization) and protein-DNA binding. This finding allows us to extend the application of this assay concept to investigate protein oligomerization or to detect mutations related to protein oligomerization.

3.5. Measurement of cellular p53 activity

To investigate nanosensor applicability in studying DNA-binding function of cellular p53, we used stably transfected H1299 cells expressing either wildtype or mutant p53 under an ecdysone inducible (EI) promoter [46]. Missense mutations in the p53-expressing *TP53* gene resulting in amino acid substitutions: R175H, G245S and R273H belong to a group of "hot-spot" mutations that are most frequently associated with human cancers [7]. While each causative mutation confers different degrees of structural defect within the well-ordered DNA-binding core domain, these mutants are largely unable to bind p53 REs, and thus p53 transcriptional activity and ensuing cellular responses are abrogated [47].

Probe_PUMA mixed with cellular lysates comprising wildtype p53 (wt) displayed an increase in hydrodynamic size in a concentration dependent manner (**Fig. S4**). This response was not observed when lysates from p53-null vehicle cells (null), or mutant p53 expressing cells (G245S, R273H and R175H) were used (**Fig. 3a**), indicating successful detection of functional p53 in cell lysates. The Western blot bands in **Fig. 3a inset** indicate that expression levels of the mutant or wildtype p53 proteins in the lysates tested were similar, except for the R175H mutant that was expressed at a slightly lower amount. Our nanoDLS assay is a functional technique that measures DNA binding ability of the p53 proteins. Mutant p53 proteins have negligible binding with Probe_PUMA leading to negligible size increase, but wildtype p53 proteins bind Probe_PUMA with high affinity which result in significant size increase as shown in **Fig. 3a**. In addition, Probe_PUMA is stable in wtp53 containing cell lysates for at least 2 h upon mixing (**Fig. S5**). The p53 binding kinetics suggest very quick and tight binding onto Probe_PUMA which conceivably protects the complex against any potential nuclease digestion, leading to enhanced probe stability in cell lysate.

3.6. Screening of p53 activating or reactivating drugs in cell lysates

Many of the commonly used genotoxic anticancer drugs elicit cellular responses that converge on p53, augmenting its activity and stabilizing protein levels in cells expressing wildtype p53 through post-translational modifications that potentiate specific DNA binding [48, 49]. Wildtype p53 expressing H1299 cells treated with three well-known anticancer drugs: actinomycin-D (ActD), doxorubicin (Dox), or etoposide (Eto) were assessed for p53 function. The average size of Probe_$_{PUMA}$ increased by 40 nm when exposed to lysate from untreated cells, and further increased in response to anticancer drug treatments, indicative of enhanced p53 activity (**Fig. 3b**).

Another class of p53-targeting therapeutics focus on wildtype p53 carrying cancers that show diminished p53 response from factors such as reduced protein expression (epigenetic silencing or diminished protein translation), increased protein turnover (overexpressed p53-targeting E3-ligases e.g., Mdm2, COP1, loss of p19ARF gene) or attenuated anti-survival pathways (e.g., increase in anti-apoptotic factors) [5, 50]. Inhibition of p53-Mdm2 interaction can prevent p53 from being targeted for proteasomal degradation, leading to rapid elevation of cellular p53 levels and activity [51]. HCT116 cells expressing endogenous wildtype p53 were treated with small molecule (Nutlin) and peptidic (sMTide-02) Mdm2 antagonists [52], and the respective cell lysates were assayed for p53-DNA binding activity. The results indicate clear elevation of p53 activity represented by the significant increase in probe size for drug-treated cells in a concentration-dependent manner (**Fig. 3c**), commensurate with the increased p53 protein levels upon drug treatment (**Fig. 3c, inset**). Furthermore, the hydrodynamic size increase was almost negligible if the cell lysate was pre-incubated with excess wtp53 binding ConA sequences (**Fig. S6**), indicating that the size increase is due to the specific interaction between the Probe_$_{PUMA}$ and cellular p53 proteins, and not due to random aggregation. As such, the nanosensor can be applied to cell-based screening of Mdm2 inhibitors, an area of significant clinical interest.

As inactivating p53 mutations are present in more than half of all cancers, a promising treatment strategy lies in the identification of therapeutics that target and restore wildtype functions to p53 mutants [53]. The R175H and R273H mutants are two of the most well-characterized 'hot-spots' mutants displaying distinct structural defects affecting DNA-binding. The R175H mutation disrupts zinc atom coordination resulting in a collapse in overall protein structure and extensive protein unfolding, whereas the R273H mutant retains wildtype p53 structure but not DNA-binding function due to the loss of critical contacts to DNA [54]. We next examined mutant p53 reactivation activity of several small molecule compounds in pre- and early-clinical trials. COTI-2 was found to exhibit anti-tumoral effects on numerous mutant p53 bearing cancer cell lines through mechanisms that are currently unclear [55]. Compound NSC319726 (ZMC1) was reported to target R175H mutant for reactivation by enhancing zinc chelation and protein folding through an increase in intracellular zinc concentrations [56, 57]. PRIMA-1^{MET} (APR246) has been described to reactivate several p53 mutants (R175H, R273H, R248Q) through covalent modifications of thiol groups on mutant proteins [58, 59]. H1299-EIp53 Cells expressing either the R175H or R273H p53 mutants were treated with each of the reactivating compounds (COTI-2, PRIMA-1^{MET} and NSC319726) [55, 57, 58] and cell lysates were assayed for p53-Probe$_{PUMA}$ binding. The results indicate reactivation of both R175H and R273H mutants by COTI-2 (1 μM) and PRIMA-1^{MET} (20 μM) (**Fig. 3d-e**). Notably, NSC319726 compound only reactivated R175H, at both low (0.3 μM) and high concentrations (3 μM) in accordance with its described R175H-specificity (**Fig. 3d**) [57] and did not reactivate the R273H mutant at both concentrations tested (**Fig. 3e**). This result shows that this nanosensor can rapidly discern mutant-specific reactivation in cellular samples, which holds much potential for high-throughput anticancer drug screening campaigns.

4. Conclusions

In summary, we have developed an ultrasensitive DLS based nanobiosensor to screen for p53 activators or reactivators in complex cellular contexts. The unique dumbbell construct of DNA-linked AuNPs with large scattering dimension not only offers excellent sensitivity (0.06 pM detection limit), but also endows it with high sequence specificity and protein selectivity with the suppression of non-binding background entities. Additionally, it allows for precise interrogation of protein function following cell-based drug treatments, providing a simultaneous secondary assessment where phenotypic screens can be immediately target-validated and genotypically addressed. This is especially helpful in forward chemical genetics approaches using chemical libraries where active compounds often display strong off-target or cytotoxic effects in-vivo [60]. This novel nanobiosensor also provides means of identifying targeted therapeutics which require intact cellular environment, intracellular chemical modifications, metabolic activation, or the presence of molecular cofactors for activity, as proven essential for proper function of several p53 reactivating compounds [56, 58, 61]. In addition, DNA response element sequences embedded in the nano-dumbbell probe can be easily modified for detecting other DNA-binding proteins and cell-based screening of their related drug candidates. This nanosensor allows a one-step "mix-and-measure" screening of drugs, affords a robust method to profile protein-DNA interactions in a label-free, sensitive and real-time manner, and will be of use for high-throughput screening of anticancer drugs.

CONFLICT OF INTEREST

The authors declare no conflict of interest.

ACKNOWLEDGEMENTS

The authors would like to acknowledge the Agency for Science, Technology and Research (A*STAR), Singapore, for financial support under JCO CDA grant 13302FG063. We thank Wayne Danter (Critical Outcome Technologies) for his kind gift of COTI-2 compound.

‡X.T. Zheng and W. L. Goh contributed equally to this work.

RFERENCES

[1] D.M. Molina, R. Jafari, M. Ignatushchenko, T. Seki, E.A. Larsson, C. Dan, et al., Monitoring Drug Target Engagement in Cells and Tissues Using the Cellular Thermal Shift Assay, Science, 341(2013) 84-7.
[2] D.C. Swinney, J. Anthony, How were new medicines discovered?, Nature Reviews Drug Discovery, 10(2011) 507.
[3] J. Hughes, S. Rees, S. Kalindjian, K. Philpott, Principles of early drug discovery, Br J Pharmacol, 162(2011) 1239-49.
[4] R. Macarron, M.N. Banks, D. Bojanic, D.J. Burns, D.A. Cirovic, T. Garyantes, et al., Impact of high-throughput screening in biomedical research, Nature Reviews Drug Discovery, 10(2011) 188.
[5] B. Vogelstein, D. Lane, A.J. Levine, Surfing the p53 network, Nature, 408(2000) 307-10.
[6] D.P. McLornan, A. List, G.J. Mufti, Applying synthetic lethality for the selective targeting of cancer, New Engl J Med, 371(2014) 1725-35.
[7] A.N. Bullock, A.R. Fersht, Rescuing the function of mutant p53, Nat Rev Cancer, 1(2001) 68-76.
[8] J. Yu, L. Zhang, P.M. Hwang, C. Rago, K.W. Kinzler, B. Vogelstein, Identification and classification of p53-regulated genes, Proc Natl Acad Sci USA, 96(1999) 14517-22.
[9] P. Hainaut, T. Hernandez, A. Robinson, P. Rodriguez-Tome, T. Flores, M. Hollstein, et al., IARC Database of p53 gene mutations in human tumors and cell lines: updated compilation, revised formats and new visualisation tools, Nucleic Acids Res, 26(1998) 205-13.
[10] M. Fried, D.M. Crothers, EQUILIBRIA AND KINETICS OF LAC REPRESSOR-OPERATOR INTERACTIONS BY POLYACRYLAMIDE-GEL ELECTROPHORESIS, Nucleic Acids Res, 9(1981) 6505-25.
[11] R.L. Weinberg, D.B. Veprintsev, A.R. Fersht, Cooperative binding of tetrameric p53 to DNA, J Mol Biol, 341(2004) 1145-59.
[12] R.L. Weinberg, D.B. Veprintsev, M. Bycroft, A.R. Fersht, Comparative binding of p53 to its promoter and DNA recognition elements, J Mol Biol, 348(2005) 589-96.
[13] N. Yang, X. Su, V. Tjong, W. Knoll, Evaluation of two- and three-dimensional streptavidin binding platforms for surface plasmon resonance spectroscopy studies of DNA hybridization and protein-DNA binding, Biosens Bioelectron, 22(2007) 2700-6.
[14] Y. Wang, X. Zhu, M. Wu, N. Xia, J. Wang, F. Zhou, Simultaneous and Label-Free Determination of Wild-Type and Mutant p53 at a Single Surface Plasmon Resonance Chip Preimmobilized with Consensus DNA and Monoclonal Antibody, Anal Chem, 81(2009) 8441-6.
[15] E. Jagelska, V. Brazda, S. Pospisilova, B. Vojtesek, E. Palecek, New ELISA technique for analysis of p53 protein/DNA binding properties, J Immunol Methods, 267(2002) 227-35.
[16] W. Goh, D. Lane, F. Ghadessy, Development of a novel multiplex in vitro binding assay to profile p53-DNA interactions, Cell Cycle, 9(2010) 3030-8.
[17] M.A. Noureddine, D. Menendez, M.R. Campbell, O.J. Bandele, M.M. Horvath, X. Wang, et al., Probing the Functional Impact of Sequence Variation on p53-DNA Interactions Using a Novel Microsphere Assay for Protein-DNA Binding with Human Cell Extracts, PLoS Genet, 5(2009).
[18] J. Yeo, J.-Y. Park, W.J. Bae, Y.S. Lee, B.H. Kim, Y. Cho, et al., Label-Free Electrochemical Detection of the p53 Core Domain Protein on Its Antibody Immobilized Electrode, Anal Chem, 81(2009) 4770-7.

[19] P. Chandra, Nanobiosensors for Personalized and Onsite Biomedical Diagnosis: Institution of Engineering and Technology; 2016.
[20] P. Chandra, H.-B. Noh, M.-S. Won, Y.-B. Shim, Detection of daunomycin using phosphatidylserine and aptamer co-immobilized on Au nanoparticles deposited conducting polymer, Biosens Bioelectron, 26(2011) 4442-9.
[21] P. Chandra, S.A. Zaidi, H.-B. Noh, Y.-B. Shim, Separation and simultaneous detection of anticancer drugs in a microfluidic device with an amperometric biosensor, Biosens Bioelectron, 28(2011) 326-32.
[22] H. Afsharan, F. Navaeipour, B. Khalilzadeh, H. Tajalli, M. Mollabashi, M.J. Ahar, et al., Highly sensitive electrochemiluminescence detection of p53 protein using functionalized Ru–silica nanoporous@gold nanocomposite, Biosensors & Bioelectronics, 80(2016) 146-53.
[23] X. Chen, C. He, Z. Zhang, J. Wang, Sensitive chemiluminescence detection of wild-type p53 protein captured by surface-confined consensus DNA duplexes, Biosens Bioelectron, 47(2013) 335-9.
[24] B. Lorber, F. Fischer, M. Bailly, H. Roy, D. Kern, Protein analysis by dynamic light scattering: Methods and techniques for students, Biochemistry and Molecular Biology Education, 40(2012) 372-82.
[25] Q. Dai, X. Liu, J. Coutts, L. Austin, Q. Huo, A One-Step Highly Sensitive Method for DNA Detection Using Dynamic Light Scattering, J Am Chem Soc, 130(2008) 8138-9.
[26] N. Seow, Y.N. Tan, L.-Y.L. Yung, X. Su, DNA-Directed Assembly of Nanogold Dimers: A Unique Dynamic Light Scattering Sensing Probe for Transcription Factor Detection, Sci Rep, 5(2015) 18293.
[27] X. Liu, Q. Dai, L. Austin, J. Coutts, G. Knowles, J. Zou, et al., A One-Step Homogeneous Immunoassay for Cancer Biomarker Detection Using Gold Nanoparticle Probes Coupled with Dynamic Light Scattering, J Am Chem Soc, 130(2008) 2780-2.
[28] H. Jans, X. Liu, L. Austin, G. Maes, Q. Huo, Dynamic Light Scattering as a Powerful Tool for Gold Nanoparticle Bioconjugation and Biomolecular Binding Studies, Anal Chem, 81(2009) 9425-32.
[29] X. Miao, S. Zou, H. Zhang, L. Ling, Highly sensitive carcinoembryonic antigen detection using Ag@Au core–shell nanoparticles and dynamic light scattering, Sensors Actuators B: Chem, 191(2014) 396-400.
[30] X. Huang, Z. Xu, Y. Mao, Y. Ji, H. Xu, Y. Xiong, et al., Gold nanoparticle-based dynamic light scattering immunoassay for ultrasensitive detection of Listeria monocytogenes in lettuces, Biosens Bioelectron, 66(2015) 184-90.
[31] H. Jans, Q. Huo, Gold nanoparticle-enabled biological and chemical detection and analysis, Chem Soc Rev, 41(2012) 2849-66.
[32] Y. Sun, H. Zhao, I. Boussouar, F. Zhang, D. Tian, H. Li, Highly sensitive chiral sensing by calix[4]arene-modified silver nanoparticles via dynamic light scattering, Sensors Actuators B: Chem, 216(2015) 235-9.
[33] D.A. Handley, Colloidal Gold: Principles, Methods, and Applications, New York: Academic Press; 1989.
[34] W.J. Qin, L.Y.L. Yung, Nanoparticle-DNA Conjugates Bearing a Specific Number of Short DNA Strands by Enzymatic Manipulation of Nanoparticle-bound DNA, Langmuir, 21(2005) 11330-4.
[35] W.J. Qin, L.Y.L. Yung, Nanoparticle-based detection and quantification of DNA with single nucleotide polymorphism (SNP) discrimination selectivity, Nucleic Acids Res, 35(2007) e111-e.
[36] W.J. Qin, L.Y.L. Yung, Nanoparticle carrying a single probe for target DNA detection and single nucleotide discrimination, Biosens Bioelectron, 25(2009) 313-9.

[37] P.M. Neilsen, J.E. Noll, R.J. Suetani, R.B. Schulz, F. Al-Ejeh, A. Evdokiou, et al., Mutant p53 uses p63 as a molecular chaperone to alter gene expression and induce a pro-invasive secretome, Oncotarget, 2(2011) 1203-17.
[38] J.E. Noll, J. Jeffery, F. Al-Ejeh, R. Kumar, K.K. Khanna, D.F. Callen, et al., Mutant p53 drives multinucleation and invasion through a process that is suppressed by ANKRD11, Oncogene, 31(2012) 2836-48.
[39] R.L. Weinberg, D.B. Veprintsev, M. Bycroft, A.R. Fersht, Comparative binding of p53 to its promoter and DNA recognition elements, J Mol Biol, 348(2005) 589-96.
[40] H.J. Ong, J.W. Siau, J.B. Zhang, M. Hong, H. Flotow, F. Ghadessy, Analysis of p53 binding to DNA by fluorescence imaging microscopy, Micron, 43(2012) 996-1000.
[41] S. Kearns, R. Lurz, E.V. Orlova, A.L. Okorokov, Two p53 tetramers bind one consensus DNA response element, Nucleic Acids Res, 44(2016) 6185-99.
[42] B. Wang, Z. Xiao, E.C. Ren, Redefining the p53 response element, Proc Natl Acad Sci USA, 106(2009) 14373-8.
[43] W. Goh, D. Lane, F. Ghadessy, Development of a novel multiplex in vitro binding assay to profile p53-DNA interactions, Cell Cycle, 9(2010) 3030-8.
[44] T. Tebaldi, S. Zaccara, F. Alessandrini, A. Bisio, Y. Ciribilli, A. Inga, Whole-genome cartography of p53 response elements ranked on transactivation potential, BMC Genomics, 16(2015) 464.
[45] A. Willis, E.J. Jung, T. Wakefield, X. Chen, Mutant p53 exerts a dominant negative effect by preventing wild-type p53 from binding to the promoter of its target genes, Oncogene, 23(2004) 2330-8.
[46] M.J. Scian, K.E.R. Stagliano, M.A.E. Anderson, S. Hassan, M. Bowman, M.F. Miles, et al., Tumor-Derived p53 Mutants Induce NF-κB2 Gene Expression, Mol Cell Biol, 25(2005) 10097-110.
[47] A.N. Bullock, J. Henckel, A.R. Fersht, Quantitative analysis of residual folding and DNA binding in mutant p53 core domain: definition of mutant states for rescue in cancer therapy, Oncogene, 19(2000) 1245-56.
[48] R.B. Tishler, S.K. Calderwood, C.N. Coleman, B.D. Price, Increases in sequence specific DNA binding by p53 following treatment with chemotherapeutic and DNA damaging agents, Cancer Res, 53(1993) 2212-6.
[49] M.L. Choong, H. Yang, M.A. Lee, D.P. Lane, Specific activation of the p53 pathway by low dose actinomycin D: a new route to p53 based cyclotherapy, Cell Cycle, 8(2009) 2810-8.
[50] V. Pant, G. Lozano, Limiting the power of p53 through the ubiquitin proteasome pathway, Genes Dev, 28(2014) 1739-51.
[51] I.M. van Leeuwen, M. Higgins, J. Campbell, C.J. Brown, A.R. McCarthy, L. Pirrie, et al., Mechanism-specific signatures for small-molecule p53 activators, Cell Cycle, 10(2011) 1590-8.
[52] C.J. Brown, S.T. Quah, J. Jong, A.M. Goh, P.C. Chiam, K.H. Khoo, et al., Stapled peptides with improved potency and specificity that activate p53, ACS Chem Bio, 8(2013) 506-12.
[53] C.J. Brown, S. Lain, C.S. Verma, A.R. Fersht, D.P. Lane, Awakening guardian angels: drugging the p53 pathway, Nat Rev Cancer, 9(2009) 862-73.
[54] A.C. Joerger, H.C. Ang, A.R. Fersht, Structural basis for understanding oncogenic p53 mutations and designing rescue drugs, Proc Natl Acad Sci USA, 103(2006) 15056-61.
[55] K.Y. Salim, S. Maleki Vareki, W.R. Danter, J. Koropatnick, COTI-2, a novel small molecule that is active against multiple human cancer cell lines in vitro and in vivo, Oncotarget, (2016).
[56] X. Yu, A.R. Blanden, S. Narayanan, L. Jayakumar, D. Lubin, D. Augeri, et al., Small molecule restoration of wildtype structure and function of mutant p53 using a novel zinc-metallochaperone based mechanism, Oncotarget, 5(2014) 8879-92.

[57] X. Yu, A. Vazquez, A.J. Levine, D.R. Carpizo, Allele-specific p53 mutant reactivation, Cancer Cell, 21(2012) 614-25.
[58] J.M. Lambert, P. Gorzov, D.B. Veprintsev, M. Soderqvist, D. Segerback, J. Bergman, et al., PRIMA-1 reactivates mutant p53 by covalent binding to the core domain, Cancer Cell, 15(2009) 376-88.
[59] V.J. Bykov, N. Issaeva, A. Shilov, M. Hultcrantz, E. Pugacheva, P. Chumakov, et al., Restoration of the tumor suppressor function to mutant p53 by a low-molecular-weight compound, Nat Med, 8(2002) 282-8.
[60] J.P. Hughes, S. Rees, S.B. Kalindjian, K.L. Philpott, Principles of early drug discovery, Br J Pharmacol, 162(2011) 1239-49.
[61] M. Hiraki, S.Y. Hwang, S. Cao, T.R. Ramadhar, S. Byun, K.W. Yoon, et al., Small-Molecule Reactivation of Mutant p53 to Wild-Type-like p53 through the p53-Hsp40 Regulatory Axis, Chem Biol, 22(2015) 1206-16.
[62] M. Brazdova, V. Tichy, R. Helma, P. Bazantova, A. Polaskova, A. Krejci, et al., p53 Specifically Binds Triplex DNA In Vitro and in Cells, PLoS One, 11(2016) e0167439.
[63] P. Balagurumoorthy, H. Sakamoto, M.S. Lewis, N. Zambrano, G.M. Clore, A.M. Gronenborn, et al., Four p53 DNA-binding domain peptides bind natural p53-response elements and bend the DNA, Proc Natl Acad Sci USA, 92(1995) 8591-5.
[64] R.L. Weinberg, S.M. Freund, D.B. Veprintsev, M. Bycroft, A.R. Fersht, Regulation of DNA binding of p53 by its C-terminal domain, J Mol Biol, 342(2004) 801-11.

Figures and captions

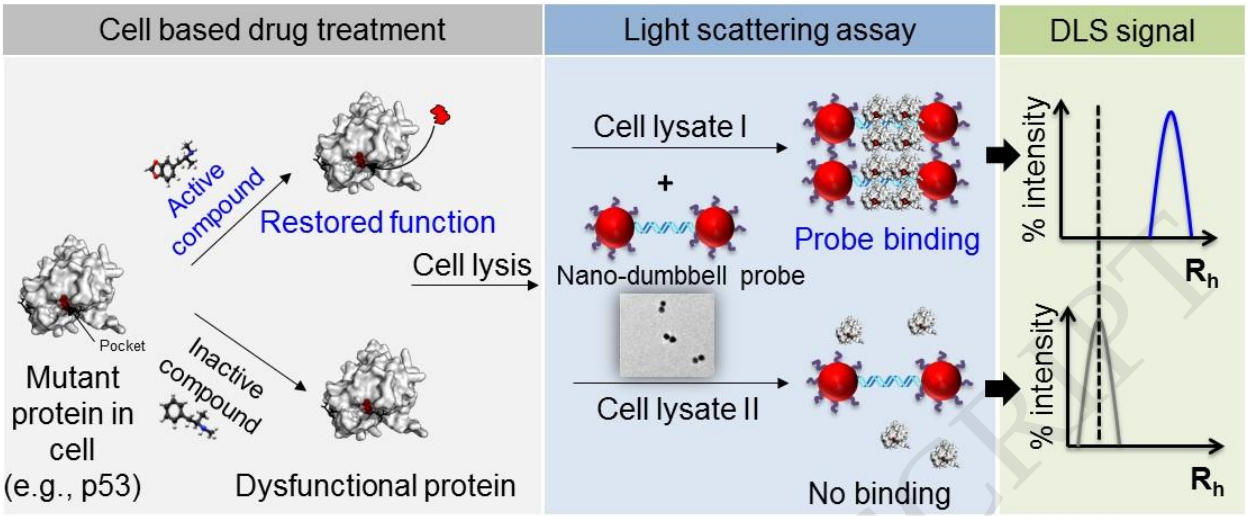

Scheme 1. Principle of dynamic light scattering based (DLS) drug screening using nano-dumbbell probes (R_h: Hydrodynamic diameter).

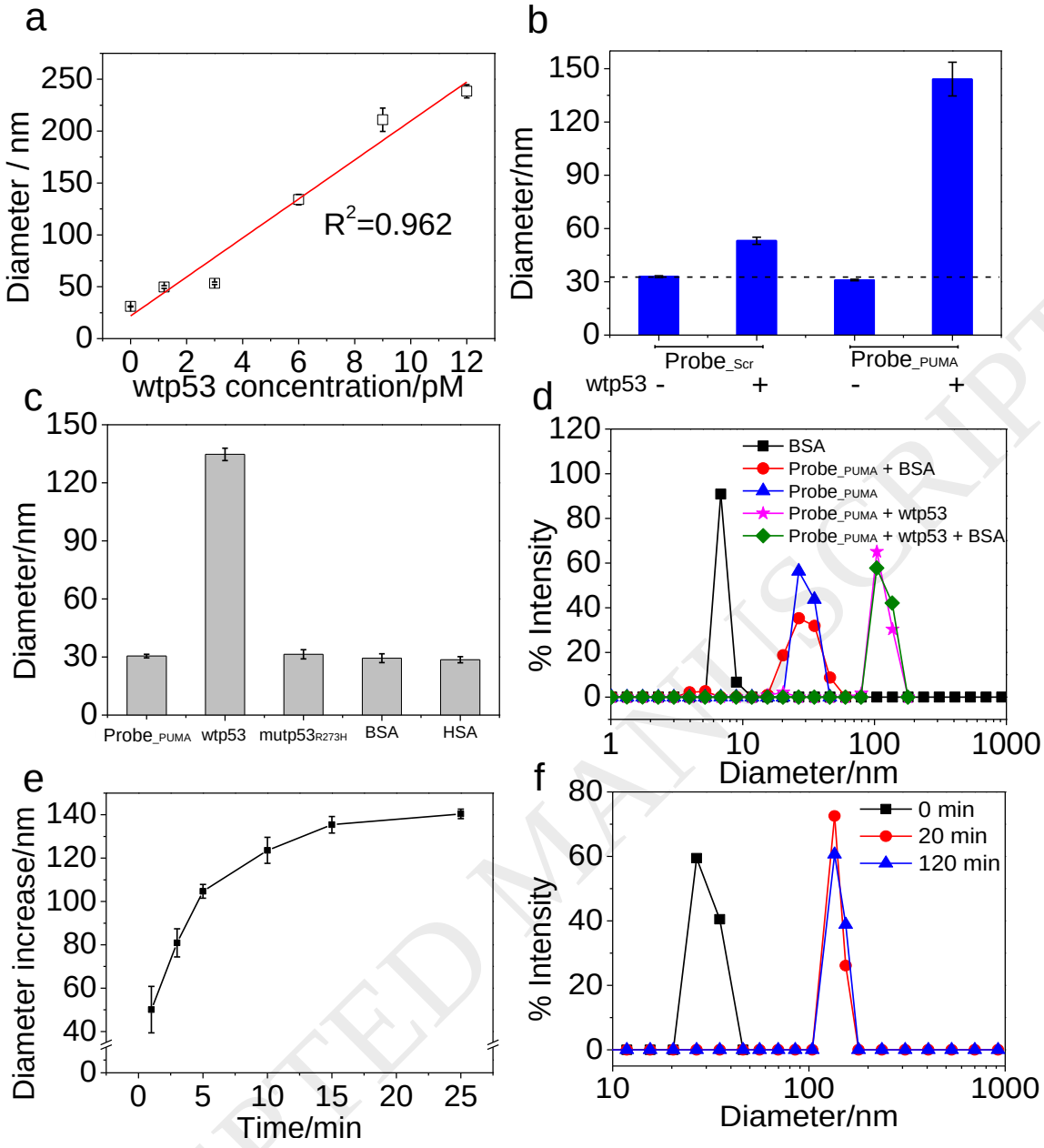

Fig. 1. (a) Linear correlation plot between average diameter and wtp53 concentration in the presence of 300 pM Probe$_{PUMA}$. (b) Respective sizes of control Probe$_{Scr}$ and Probe$_{PUMA}$ showing sequence-specific DNA binding of wtp53 to Probe$_{PUMA}$. Black-hashed line show baseline of unbound probes. wtp53 + and - signs indicate the presence or absence of wtp53 proteins, respectively. (c) Average size of Probe$_{PUMA}$ in the presence of wtp53, DNA-binding deficient mutp53$_{R273H}$, or non-specific proteins (BSA and HSA). (d) Size distribution plots of BSA only (black square), Probe$_{PUMA}$ with or without BSA (red dot and blue triangle, respectively), and wtp53-bound Probe$_{PUMA}$ with or without BSA (green diamond and pink star, respectively). Errors depict S.D. of 3 individual binding reactions for all experiments. (e) Real-time DLS measurement of wtp53 and Probe$_{PUMA}$ binding. (f) Size distribution plots of Probe$_{PUMA}$ before (0 min, black square) and after addition of wtp53 for 20 min (red dot) and 120 min (blue triangle) respectively.

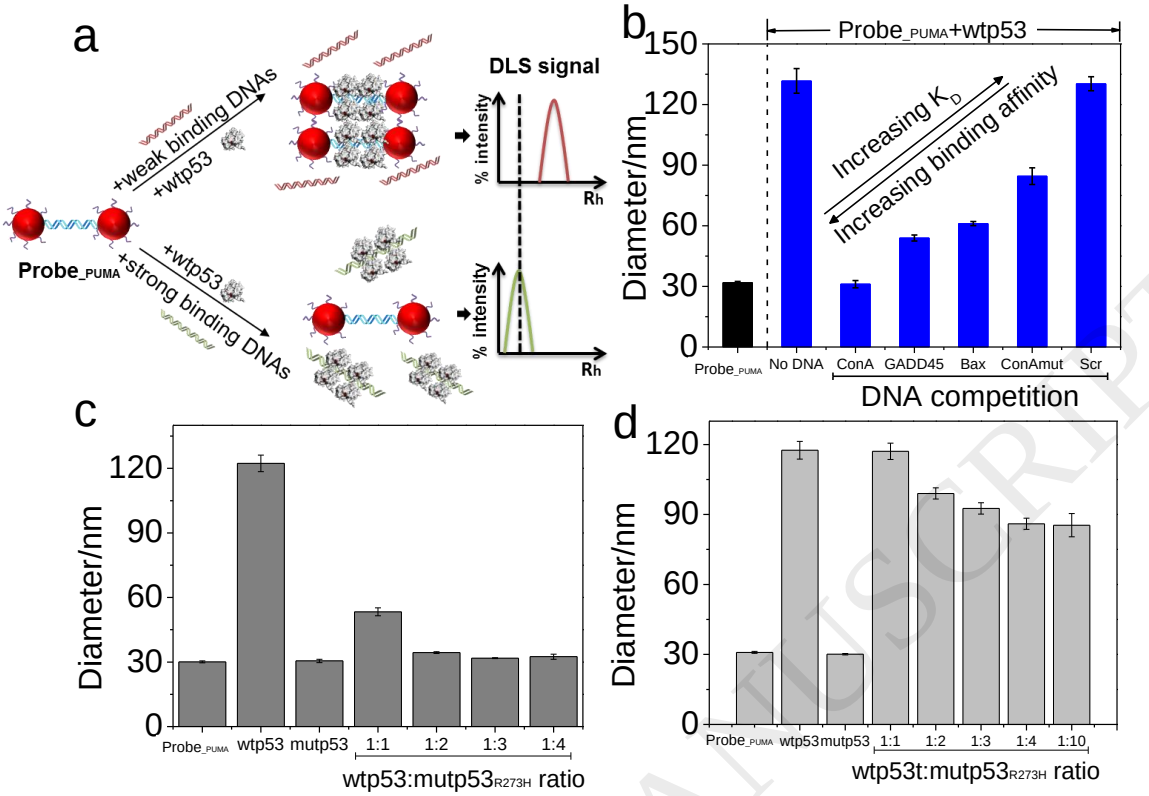

Fig. 2. (a) A competitive assay design to determine the relative binding affinity of wtp53 proteins towards different REs. In this assay, wtp53 proteins were preincubated with optimized amount of Probe_PUMA and a large excess of competing free DNA oligonucleotides in one pot (~3300-fold higher in concentration than Probe_PUMA). (b) Statistical analysis indicates that the higher the binding affinity of the free DNA RE sequences, the smaller the diameter of Probe_PUMA due to effective competition. (c-d) p53-Probe_PUMA binding showing dominant negative effects of mutp53$_{R273H}$ proteins at increasing proportions to wtp53 when exposed to Probe_PUMA either (c) after 20 min pre-incubation, or (d) simultaneously. Errors depict S.D. of 3 individual binding reactions for all experiments.

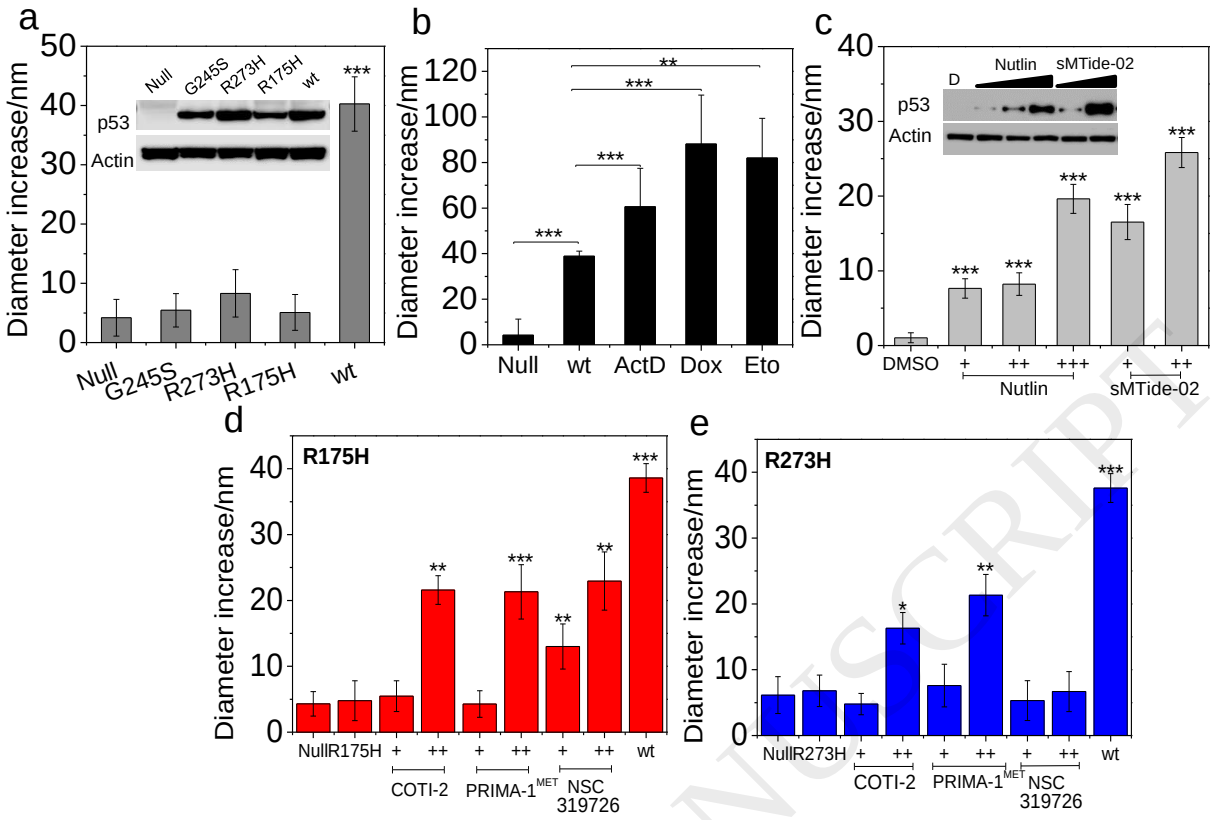

Fig. 3. Analysis of p53-DNA binding in whole-cell lysates. (a) Hydrodynamic size change of Probe$_{PUMA}$ when added to H1299-EIp53 cells carrying either vehicle cassette (Null), or inducible constructs expressing either wildtype (wt), or mutant p53 (R273H, G245S, R175H) proteins. Western blot inset shows respective p53 protein levels. (b) Increase in DNA binding activity of cellular wildtype p53 from cells pre-treated with DMSO control, 2 nM Actinomycin-D, 0.5 μM Doxorubicin, or 5 μM Etoposide for 24 hours. (c) Probe$_{PUMA}$ size change after exposure to cellular lysates of wildtype p53-expressing HCT116 cells treated with Nutlin (1 μM (+), 4 μM (++), 10 μM (+++)) or sMTide-02 staple peptide (5 μM (+), 20 μM (++)). Western blot inset shows respective p53 protein levels. (d-e) Analysis of reactivation of p53-DNA binding in H1299-EIp53 cells. Probe$_{PUMA}$ size change after exposure to cellular lysates of either (d) R175H, or (e) R273H mutant p53-expressing cells treated with COTI-2 (0.2 μM, 1 μM), PRIMA-1^{MET}/APR246 (5 μM, 20 μM) or NSC319726/ZMC1 (0.3 μM, 3 μM). + and ++ indicate the low or high concentrations of each compound added, respectively. Errors depict S.D. of 3 individual binding reactions for all experiments. Two-tailed student's t-tests were performed to assess statistical significance (*p<0.05, **p<0.01, ***p<0.001).